Solution of the Pure Metals Solidification Problem by Involving the Material Shrinkage and the Air-Gap Between Material and Mold

J. Matlak, D. Słota*

Institute of Mathematics, Silesian University of Technology,
Kaszubska 23, 44-100 Gliwice, Poland
*Corresponding author. E-mail address: damian.slota@polsl.pl

Abstract

In this paper we describe an algorithm for solving the pure metals solidification problem by involving the metal shrinkage and air-gap between material and mold. In this algorithm we use the finite element method supplemented by the procedures allowing to define the position of the moving interface and the change of the material size associated with the shrinkage. We present also an example illustrating the precision of presented method.

1. Introduction

The Stefan problem [1-3] consists in determining the temperature distribution in the liquid and solid phases. Simultaneously, the position of boundary between the phases should be found as well. In easy cases it is possible to find the exact solution of the Stefan problem [4, 5], but generally to find its solution the numerical or numerical-analytical methods must be used. In paper [6] the Green element method has been employed to solve a one-dimensional one-phase Stefan problem by adopting an enthalpy formulation. Yoon in paper [7] presents the explicit and implicit extended moving least squares difference methods for solving one-dimensional Stefan problem. In the paper [8] a numerical methodology based on the curvilinear, boundary-fitted, finite-volume method for solidification and melting problems for pure substances based on moving grids is developed.

Kim in paper [9] present two simple numerical methods to find the free boundary in one-phase Stefan problem. He use a log-transform function with the unfixed and fixed free boundary. Qu et all in paper [10] solve one-dimensional phase change problem with periodic boundary condition by using an invariant-space-grid to finite difference method. The papers [11-15] presents an analytic method applied for finding the approximate solution of Stefan problem reduced to the one-phase solidification problem. Proposed method is based on the known formalism of initial extension of a sought function describing the temperature field into the power series, some coefficients of which can be determined with the aid of boundary conditions, and also based on the approximation of a function defining the freezing front location with the broken line, parameters of which can be obtained by solving the appropriate differential equations. In the papers [16-18] to solve the Stefan problem the heat balance

method and its' modifications were used. Reviews of some trends and approaches to the integral method are given in the papers [16, 19]. Numeric models for the heat transfer problems are considered also in papers [20-32].

Mathematical model for describing processes involving the simultaneous heat and mass transfer with the phase transition in foods undergoing the volume change (shrinkage or expansion) is presented in paper [33]. To approximate solution of the problem the finite element method and the Arbitrary Lagrangian-Eulerian method were used. Natale et al. in paper [34] determined the temperature distribution of the solid and liquid one-dimensional regions and the position of the two free boundaries in the solidification process with either shrinkage or expansion. The results were obtained for three different boundary conditions. In all cases, the explicit solution was given by a parametric representation of the similarity type. The one-dimensional solidification of the pure metals problem involving the metal shrinkage was considered also in paper [35]. To find the solution the perturbation method for the small Stefan numbers was used.

In this paper we present a method allowing to find the approximate solution of the pure metals solidification problem taking into account the metal shrinkage and formulation of the air-gap between mold and ingot. This method bases on the finite elements method extended with procedures that determine the position of the boundary between phases and the size of the material resulting from the shrinkage. Further we present an computational example to illustrate the precision of presented method.

2. Formulation of the problem

We will consider the solidification of pure metal in mold. In our calculations we will involve the change of metal's volume in the solid state consequential to the difference between density in solid and liquid state. We will take into account the air-gap formed between the ingot and mold. To describe the temperature distribution we used the Stefan problem. We assumed, that the cooling conditions on mold's boundary are described by the third-type boundary condition. On the contact boundary between mold and ingot the fourth-type boundary condition is given. At the beginning, before the air-gap is formed, with perfect contact. After the formation of air-gap - with thermal resistance. In the ingot's axis the heat flux density (the second-type boundary condition) is given.

We will examine the one-dimensional problem. It can be used to describe in simplified way the phenomena occurring among others inside the solidifying metal slab with height h, length l and thickness $d(t)$ ($d(t) \ll h$ and $d(t) \ll l$).

Let us consider the system of differential equations describing the solidification of the pure metal in the mold. The ingot area will be represented by the interval $\Omega_m = (0, d(t))$, that can be divided into two subintervals $D_1 = (0, \xi(t))$ and $D_2 = (\xi(t), d(t))$, representing correspondingly the liquid and the solid phase. The mold area will be represented by the interval $D_3 = (d_0, b_0)$, where d_0 and b_0 $(0 < d_0 < b_0)$ are known constants while $d(t)$ and $\xi(t)$ ($0 \leq \xi(t) \leq d(t) \leq d_0$) are unknown functions describing respectively position of the moving interface

between phases and length of the ingot area. The heat transfer equations are given [35]:

$$c_i \varrho_i \frac{\partial u(x,t)}{\partial t} = \lambda_i \frac{\partial^2 u(x,t)}{\partial x^2} + w_i \left(1 - \frac{\varrho_1}{\varrho_2}\right) \frac{d\xi(t)}{dt} \frac{\partial u(x,t)}{\partial x}, \quad (1)$$

for $(x,t) \in D_i \times (0, t^*)$, $i = 1, 2, 3$, where $i = 1$ for the liquid phase, $i = 2$ for the solid phase and $i = 3$ for the form, $w_1 = w_3 = 0$, $w_2 = 1$, c_i is the specific heat, λ_i is the thermal conductivity coefficient, ϱ_i denotes density of the corresponding phase and $1 - \frac{\varrho_1}{\varrho_2}$ is the shrinkage factor.

On the moving interface the condition of temperature continuity and the Stefan condition are defined

$$u(\xi(t), t)^+ = u(\xi(t), t)^- = u^*, \quad (2)$$

$$\kappa \frac{d\xi(t)}{dt} = \lambda_2 \frac{\partial u(x,t)}{\partial x}\bigg|_{x=\xi(t)}^+ - \lambda_1 \frac{\partial u(x,t)}{\partial x}\bigg|_{x=\xi(t)}^-, \quad (3)$$

where u^* is the phase change temperature and κ describes the latent heat of solidification per volume unit.

On the boundaries of the ingot and the mold the second and third kind boundary conditions are given:

$$-\lambda_1 \frac{\partial u(0,t)}{\partial x} = q(t), \ t \in (0, t^*), \quad (4)$$

$$-\lambda_3 \frac{\partial u(b_0,t)}{\partial x} = \alpha(u(b_0, t) - u_\infty), \ t \in (0, t^*), \quad (5)$$

where α is the heat transfer coefficient and u_∞ denotes the ambient temperature. On the contact boundary between ingot and mold the fourth-type condition is given. Before formation of the air-gap, with perfect contact:

$$-\lambda_1 \frac{\partial u(d_0,t)}{\partial x}\bigg|^- = -\lambda_3 \frac{\partial u(d_0,t)}{\partial x}\bigg|^+, \ t \in (0, t_0), \quad (6)$$

whereas after the air-gap is formed, with thermal resistance:

$$-\lambda_2 \frac{\partial u(d(t),t)}{\partial x} = \frac{u(d(t),t) - u(d_0,t)}{R} = -\lambda_3 \frac{\partial u(d_0,t)}{\partial x}, \ t \in (t_0, t^*), \quad (7)$$

where $R = \frac{\lambda_s}{d_0 - d(t)}$ denotes the resistance of the air-gap, λ_s is the thermal conductivity coefficient of air-gap, t_0 is the moment of the air-gap formation. For the unknown functions u, ξ and d we have to give the initial conditions:

$$u(x, 0) = u_0(x), \quad (8)$$

$$\xi(0) = \xi_0, \quad (9)$$

$$d(0) = d_0, \quad (10)$$

where u_0, ξ_0 and d_0 are given.

3. Method of solution

In this section we will describe the method of finding the solution of the problem given above. First we will present a procedure of determining the size of the ingot area. Further we will describe the method of meshing the spatial dimension and finding the time step sizes. At the end we will mention the way of using the finite elements method in our algorithm.

Assume, that the ingot has the constant mass equal to the initial mass m_0. According to the mass balance the sum of masses of the liquid and solid state is equal to m_0, i.e.:

$$m_s + m_l = m_0. \tag{11}$$

Assuming, that the densities ϱ_1 and ϱ_2 of the solid and liquid phases are constant, the above equation takes the form:

$$\varrho_1 \xi(t) + \varrho_2 \big(d(t) - \xi(t) \big) = \varrho_1 \xi_0 + \varrho_2 (d_0 - \xi_0). \tag{12}$$

If we additionally assume, that in initial moment the whole ingot is in the liquid state ($\xi_0 = d_0$) we can determine the material length function $d(t)$ as [36]:

$$d(t) = \frac{\varrho_1}{\varrho_2} \big(d_0 - \xi(t) \big) + \xi(t). \tag{13}$$

In moment t_k we divide the ingot area to n_m and the form area to n_3 elements, using $n + 2$ ($n = n_m + n_3$) nodes:

$$0 = x_0^k < \cdots < x_{n_m}^k = d(t_k) \leq$$
$$\leq d_0 = x_{n_m+1}^k < \cdots < x_{n+1}^k = b_0. \tag{14}$$

In our method we require the boundary between the liquid and solid phase to move between the adjacent nodes, starting from the node $x_{n_m}^0$, i.e. in the moment t_k the boundary will be in the node $x_{n_m-k}^k = \xi(t_k)$. To simplify the computations divide the area Ω_m to the elements with equal weight. The length between nodes will be then constant in each phase and equal to:

$$h_1 = \frac{d_0}{n_m}, \qquad \text{for the liquid phase,} \tag{15}$$

$$h_2 = \frac{\varrho_2}{\varrho_1} \frac{d_0}{n_m}, \quad \text{for the solid phase,} \tag{16}$$

$$h_3 = \frac{b_0 - d_0}{n_3}, \quad \text{for the mold.} \tag{17}$$

Let us denote $u_{i,k} = u(x_i^k, t_k)$ and $u^k = \big[u_{0,k}, \dots, u_{n+1,k} \big]^T$.

We will now describe the procedure of determining the time step size. The initial time step size can be obtained from the Stefan condition for $t = 0$:

$$\Delta t = \frac{-\kappa h_1}{\lambda_3 \frac{u_{n_m+2,0} - u_{n_m+1,0}}{h_3} - \lambda_1 \frac{u^* - u_{n_m-1,0}}{h_1}}. \tag{18}$$

After determining the temperature distribution in moment t_k we may correct the time step size using the following equations (also resulting from the Stefan condition):

$$\Delta t = \frac{-\kappa h_1}{\lambda_2 \frac{u_{n_m-k+1,k} - u^*}{h_2} - \lambda_1 \frac{u^* - u_{n_m-k-1,k}}{h_1}} \tag{19}$$

for $k < n_m$ and

$$\Delta t = \frac{-\kappa h_1}{\lambda_2 \frac{u_{1,n_m} - u^*}{h_2} - q(t_{n_m})} \tag{20}$$

for $k = n_m$. Repeat the correction until the demanded accuracy is reached.

The distribution of temperature in moment $t_{k+1} = t_k + \Delta t$ is determined using the Finite Elements Method. In this method we solve the matrix equation [2, 37]:

$$Cu' = Ku + f, \tag{21}$$

where C is the heat capacity matrix and K is the heat conductivity matrix. Matrices C, K and vector f are obtained using the Galerkin method [37] taking into account the component resulting from the convective component in equation (1) for the solid phase. The movement of the boundary between the adjacent nodes makes these matrices to be recalculated for every k. Using the implicit scheme we discretize the equation (21) to obtain the following system of the linear equations

$$\left(\frac{1}{\Delta t} C + K \right) u^{k+1} = \frac{1}{\Delta t} C u^k + f, \tag{22}$$

solution of which is the sought distribution of temperature in moment t_{k+1}.

4. Computational example

Let us consider the theoretical example with known exact solution. Assume: $c_1 = 2$, $c_2 = 4$, $c_3 = 3$, $\lambda_1 = 5$, $\lambda_2 = 3$, $\lambda_3 = \frac{100}{153}$, $\varrho_1 = 0.9$, $\varrho_2 = 1$, $\varrho_3 = \frac{41}{153}$, $\kappa = 2.3$, $u^* = 0$, $\alpha = 1$, $\xi_0 = d_0 = 1$, $b_0 = 1.1$, $t^* = 1$ and

$$q(t) = 1.8 e^{0.36(t-1)},$$

$$u_\infty(t) = 1 - 9.2\, e^{1.23(0.1+t)},$$

$$\lambda_s(t) = t \left(1 - \frac{\varrho_1}{\varrho_2} \right),$$

$$u_0(x) = \begin{cases} 1 - e^{0.36(x-1)}, & \text{for } x \leq d_0, \\ 1 - 5.1\, e^{1.23(x-1)}, & \text{for } d_0 < x \leq b_0. \end{cases}$$

Exact solution is given by functions:

$$d(t) = 1 - 0.1\, t,$$

$$\xi(t) = 1 - t,$$

$$u(x,t) = \begin{cases} 1 - e^{0.36(x+t-1)}, & \text{for } 0 \leq x < \xi(t), \\ 1 - e^{\frac{41}{30}(x+t-1)}, & \text{for } \xi(t) \leq x \leq d(t), \\ 1 - 5.1 e^{1.23(x+t-1)}, & \text{for } d_0 \leq x \leq b_0. \end{cases}$$

Calculations were performed for the grid dividing the area Ω_m to 50, 100, 200 and 500 linear elements and the area D_3 correspondingly to 5, 10, 20 and 50 elements. The required time step size precision was set $\varepsilon = 0.0001$ and was obtained on average 2 iterations.

Table 1.
Calculations' results for different grid densities (n_m - number of elements, Δ_{max} - maximal absolute error of the simulated time step, Δ_{avg} - average absolute error of the simulated time step, t^* - simulated time of completion of the process)

n_m	Run time [s]	Δ_{max}	Δ_{avg}	t^*
50	0.070	0.0394	0.0166	0.961
100	0.436	0.0346	0.0139	0.965
200	5.551	0.0322	0.0126	0.968
500	191.789	0.0307	0.0118	0.969

Table 1 presents the run time of algorithm, average and maximal time step size determination absolute error and obtained final time for each grid.

The plots presented on the figures were prepared for $n_m = 200$. Figure 1 shows the temperature curves in the ingot area in points $x_p = 0$ (dotted), 0.7 (dot-dashed) and $d(t)$ (dashed), Figure 2 shows the temperature curves in the mold area in points $x_p = 1$ (dotted), 1.05 (dot-dashed) and 1.1 (dashed). The solid lines represents the exact solution. Figure 3 shows the position of the moving interface, Figure 4 shows the length of the ingot area. The dashed lines represent the simulated values, the solid lines represent the exact solution.

The calculations' errors are caused mainly by the approximation of the derivatives on the boundary between phases appearing in the Stefan condition. It has an influence on accuracy of determining the time step based on Stefan condition. From the attached pictures we can deduce, that using the simplest linear elements allows to gain very good results. In the future we plan to use other types of elements, that will allow more accurate approximation of the temperature derivatives on the boundary between phases.
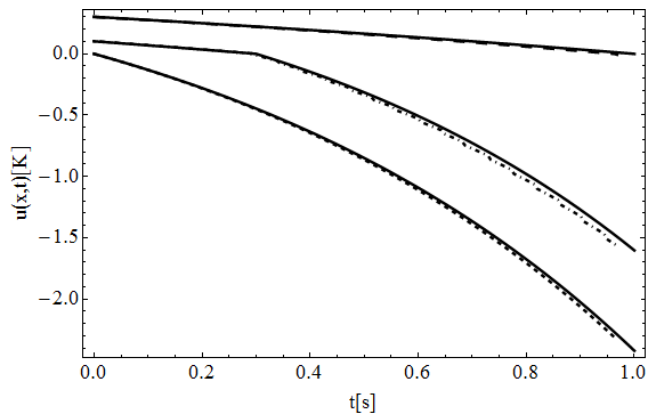

Fig. 1. The temperature curves in the ingot area in points $x_p = 0$ (dotted), 0.7 (dot-dashed) and $d(t)$ (dashed). Solid lines represent the exact solution
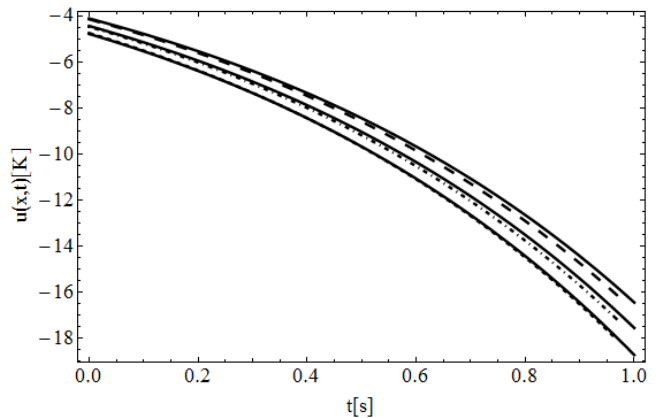

Fig. 2. The temperature curves in the mold area in points $x_p = 1$ (dotted), 1.05 (dot-dashed) and 1.1 (dashed). Solid lines represent the exact solution
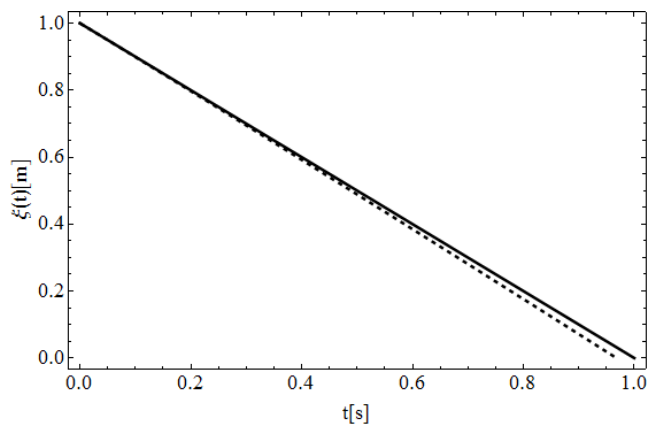

Fig. 3. Simulated (dotted) and exact (solid) position of the moving interface
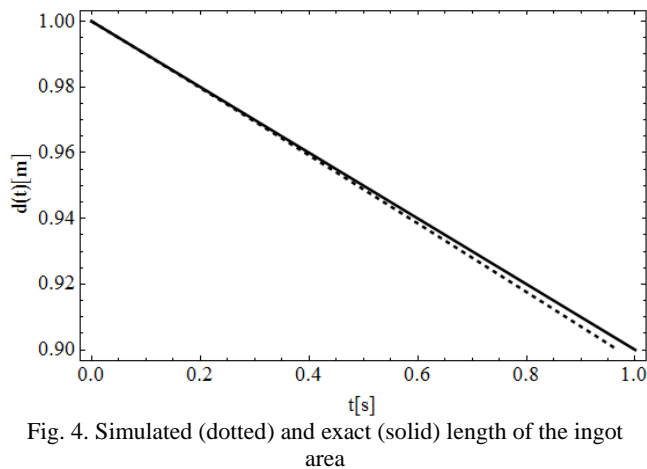
Fig. 4. Simulated (dotted) and exact (solid) length of the ingot area

5. Conclusions

In this paper we have presented the method of solving the solidification of the pure metals problem involving the material shrinkage and air-gap between material and mold. To determine the distribution of temperature we have used the finite elements method. The time step size was determined by the iterative procedure basing on the formula obtained from the Stefan condition. The length of the material in mold was obtained from the mass balance equation.

Increasing the grid density we obtain more accurate simulations, but run time of the algorithm increases incomparably fast compared to the increase of accuracy.

In the future we plan to use other types of elements to gain more accurate results. We also plan to consider the inverse issues for presented direct problem and to expand the model to multidimensional case.

References

[1] Gupta, S.C. (2003). *The Classical Stefan Problem. Basic Concepts, Modelling and Analysis*. Amsterdam. Elsevier.

[2] Mochnacki, B. Suchy, J.S. (1995). *Numerical Methods in Computations of Foundry Processes*. Cracov. PFTA.

[3] Özişik, M.N. (1993). *Heat Conduction*. New York. Wiley & Sons.

[4] Voller, V. & Falcini, F. (2013). Two exact solutions of a Stefan problem with varying diffusivity. *Int. J. Heat Mass Transfer. 58*. 80-85.

[5] Zhou, Y. Wang, Y. & Bu, W. (2014). Exact solution for a Stefan problem with latent heat a power function of position. *Int. J. Heat Mass Transfer 69*. 451-454.

[6] Onyejekwe, O. & Onyejekwe, O. (2011). Numerical solutions of the one-phase classical Stefan problem using an enthalpy green element formulation. *Adv. Eng. Soft. 42*, 743-749.

[7] Yoon, Y. (2011). Explicit and implicit extended MLS difference methods for Stefan problems. *Procedia Eng. 14*, 2751-2755.

[8] Jana S., Ray, S. & Durst, F. (2007). A numerical method to compute solidification and melting processes. *Appl. Math. Modelling 31*, 93-119.

[9] Kim, S. (2014). Two simple numerical methods for the free boundary in one-phase Stefan problem. *J. Appl. Math. 2014*. article ID 764532, 10 pages.

[10] Qu, L.-H. Ling, F. & Xing, L. (2013). Numerical study of one-dimensional Stefan problem with periodic boundary conditions, *Thermal Science 17,* 1453-1458.

[11] Hetmaniok, E. & Pleszczyński, M. (2011). Analytical method of determining the freezing front location. *Zeszyty Naukowe Politechniki Śląskiej, Matematyka Stosowana 1*, 121-136.

[12] Hetmaniok, E. & Pleszczyński, M. (2012). Application of the analytic-numerical method in solving the problem with moving boundary. *Zeszyty Naukowe Politechniki Śląskiej, Matematyka Stosowana 2*, 57-74.

[13] Grzymkowski, R., Hetmaniok, E. & Pleszczyński, M. (2011). Analytic-numerical method of determining the freezing front location. *Arch. Foundry Eng. 11*, 75-80.

[14] Grzymkowski, R., Hetmaniok, E. & Pleszczyński, M. (2013). Problem of the moving boundary in continuous casting solved by the analytic-numerical method, *Arch. Foundry Eng. 13*, 33-38.

[15] Grzymkowski, R., Hetmaniok, E., Pleszczyński, M. & Słota, D. (2013). A certain analytical method used for solving the Stefan problem, *Thermal Science 17*, 635-642.

[16] Mitchell, S.L. & Myers, T.G. (2010). Application of standard and refined heat balance integral methods to one-dimensional Stefan problems, *SIAM Rev. 52*, 57-86.

[17] Myers, T. & Mitchell, S. (2011). Application of the combined integral method to Stefan problems, *Appl. Math. Modelling 35*, 4281-4294.

[18] Layeni, O. & Johnson, J. (2012). Hybrids of the heat balance integral method, *Appl. Math. Comput. 218*, 7431-7444.

[19] Hristov, J. (2009). The heat-balance integral method by a parabolic profile with unspecified exponent: analysis and benchmark exercises, *Thermal Science 13*, 27-48.

[20] Szopa, R. & Siedlecki, J. (2010). Application of standard and refined heat balance integral methods to one-dimensional Stefan problems, *SIAM Rev. 52*, 394-354.

[21] Mochnacki, B. & Ciesielski, M. (2002). Micro/macro model of solidification using the control volume method, *Arch. Foundry 2* (4), 161-166.

[22] Suchy, J.S. & Mochnacki, B. (2003). Analysis of segregation process using the broken line model. Theoretical base, *Arch. Foundry 3* (10), 229-234.

[23] Ciesielski, M., Mochnacki, B. & Suchy, J.S. (2004). Numerical model of axiallysymmetrical casting solidification. Part I, *Arch. Foundry 4* (14), 110-113.

[24] Majchrzak, E. & Mendakiewicz, J. (2007). Gradient method of cast iron latent heat identification, *Arch. Foundry Eng. 7* (4), 121-126.

[25] Majchrzak, E., Mochnacki, B. & Kałuża, G. (2007). Shape sensitivity analysis in numerical modelling of solidification, *Arch. Foundry Eng. 7* (4), 115-120.

[26] Mochnacki, B., Majchrzak E. & Szopa, R. (2008). Simulation of heat and mass transfer in domain of casting made from binary alloy, *Arch. Foundry Eng. 8* (4), 121-126.

[27] Piasecka Belkhayat, A. (2008). Numerical modelling of solidification process using interval boundary element method, *Arch. Foundry Eng. 8 (4),* 171-176.

[28] Brociek, R., Hetmaniok, E., Matlak, J. & Słota, D. (2014). Solving of the two-dimensional unsteady heat transfer problem by using the homotopy analysis method, *Zeszyty Naukowe Politechniki Śląskiej, Matematyka Stosowana 4,* 89-102.

[29] Hetmaniok, E., Pleszczyński, M., Słota, D. & Zielonka, A. (2014). Usage of the homotopy analysis method for determining the temperature in the castingmould system, *Hutnik 81* (1), 50-54.

[30] Hetmaniok, E., Słota, D. & Zielonka, A. (2014). Solution of the inverse continuous casting problem with application of the invasive weed optimization algorithm, *Computer Methods in Materials Science 14,* 114-122.

[31] Hetmaniok, E., Słota, D.& Zielonka, A. (2014). Experimental verification of selected artificial intelligence algorithms used for solving the inverse Stefan problem, *Numer. Heat Transfer B 66,* 343-359.

[32] Hetmaniok, E., Słota, D. & Zielonka, A. (2015) Using the swarm intelligence algorithms in solution of the two-dimensional inverse Stefan problem, *Comput. Math. Appl. 69,* 347-361.

[33] Purlis, E. & Salvadori, V. (2010). A moving boundary problem in a food material undergoing volume change - simulation of bread baking. *Food Research International 43,* 949-958.

[34] Natale, M., Marcusa, E. & Tarzia, D. (2010) Explicit solutions for one-dimensional two-phase free boundary problems with either shrinkage or expansion, *Nonlinear Anal.: Real World Appl. 11,* 1946-1952.

[35] Yang, Z., Sen, M. & Paolucci, S. (2003). Solidification of a finite slab with convective cooling and shrinkage, *Appl. Math. Modelling 27,* 733-762.

[36] Matlak J. & Słota D., (accepted) Solution of the Stefan Problem by Involving the Material Shrinkage, *Czasopismo Techniczne.*

[37] Grzymkowski, R. Kapusta, A. Nowak, I. Słota, D. (2009). *Numerical Methods. The Initial-Boundary Value Problems.* Gliwice. WPKJS (in Polish)